Relationships Between Amplitudes and Kinetics of Rapid Cytosolic Free Calcium Fluctuations in GH_4C_1 Rat Pituitary Cells: Roles for Diffusion and Calcium-Induced Calcium Release

Kenneth D. Brady,* Kimberly A. Wagner,‡ Armen H. Tashjian, Jr.,*‡ and David E. Golan‡§

*Department of Molecular and Cellular Toxicology, Harvard School of Public Health; ‡Department of Biological Chemistry and Molecular Pharmacology, Harvard Medical School; and §Department of Medicine, Harvard Medical School, and Hematology-Oncology Division, Brigham and Women's Hospital, Boston, Massachusetts 02115 USA

ABSTRACT We have examined statistical relationships between the amplitudes and the kinetics (rise times, fall times, and decay constants) of cytosolic free calcium fluctuations (spikes) in a population of 353 individual GH_4C_1 rat pituitary cells. The fast falling phase was approximated by a single exponential decay, and the decay time constant, τ, increased linearly with spike amplitude in 80% of the cells studied. The slope of the τ versus amplitude plot for each cell was inversely related to the cell's mean spike amplitude. Thus, some process responsible for prolonging the decay phase of spikes appeared to operate strongly in cells with spikes of low amplitude, but to become less prominent in cells with high amplitude spikes. Mean τ correlated more strongly with mean rise and fall times than with mean spike amplitude, indicating that the kinetic properties of spikes were not tightly coupled to spike amplitude. These findings are consistent with a model wherein the rise phase corresponds to entry of extracellular calcium via L-type calcium channels into localized sub-plasmalemmal domains, followed by diffusion of sub-plasmalemmal calcium into the cell interior; and the falling phase corresponds to further calcium diffusion combined with activation of cytoplasmic calcium-induced calcium release, which prolongs the falling phase.

INTRODUCTION

Calcium ions are important in the regulation of a wide variety of cellular metabolic functions, and cytosolic free calcium concentrations are therefore tightly regulated (Stojilkovic and Catt, 1992; Berridge, 1993). GH_4C_1 cells are a clonal strain of rat pituitary somatolactotrophs (Tashjian et al., 1968) in which calcium is known to regulate prolactin secretion (Ostlund et al., 1978; Pachter et al., 1988) and synthesis (White et al., 1981). GH_4C_1 cells are excitable (Taraskevich and Douglas, 1980), containing voltage-gated calcium channels which undergo both spontaneous and inducible (Ozawa and Kimura, 1979; Taraskevich and Douglas, 1980) action potentials mediated by calcium currents. These cells also display spontaneous fluctuations or spikes (Wagner et al., 1993) in $[Ca^{2+}]_i$, and the occurrence of calcium action potentials has been shown to coincide with the initiation of these $[Ca^{2+}]_i$ fluctuations (Chiavaroli et al., 1992). The spontaneous calcium spikes are asymmetric, having rising phases which last ~0.5 s, and falling phases with mean duration of 1.7 s (K. Brady, unpublished observations). By comparison, the total duration of calcium action potentials is most often less than 200 ms (Simasko, 1991). The kinetic differences between these two events suggests that, although calcium fluctuations may be initiated by action potentials, other processes must contribute to the relatively long lifetime of the calcium fluctuations.

Our laboratory recently reported the use of the calcium indicator dye Fluo-3 (Tsien, 1989) and an interactive laser cytometer to observe calcium spikes in GH_4C_1 cells with excellent temporal resolution and signal/noise ratio (Wagner et al., 1993). The quality of these measurements was sufficiently high to allow the application of statistical methods to probe kinetic properties of the calcium spikes and to examine the manner in which spike kinetics are related to spike amplitude. We have developed a computer program, CaScan (Brady et al., manuscript in preparation), which utilizes an automated event recognition algorithm to facilitate the statistical study of calcium spike profiles. In this report, we present evidence that the durations of the rising and falling phases of calcium spikes are determined both by calcium diffusion and by involvement of a positive feedback mechanism, probably calcium-induced calcium release (CICR), which amplifies the spike magnitude and prolongs the falling phase.

MATERIALS AND METHODS

Measurement of Fluo-3 fluorescence in individual GH_4C_1 cells

GH_4C_1 cell culture (Tashjian, 1979) and preparation of cells for fluorescence measurements were performed as described previously (Wagner et al., 1993). Briefly, 48 h before an experiment, cells were plated on glass coverslips coated with Cell-Tak (Collaborative Research, Bedford, MA). On the day of an experiment, cells were rinsed with Hanks' balanced salt solution (HBSS; 118.0 mM NaCl, 4.6 mM KCl, 1.0 mM $CaCl_2$, 10 mM D-glucose, 20 mM HEPES, pH 7.40) and loaded with 9 μM Fluo-3 AM (Molecular Probes, Eugene, OR) in HBSS containing 0.04% Pluronic F-127 (Molecular

Received for publication 23 August 1993 and in final form 1 February 1994.

Address reprint requests to Dr. Kenneth D. Brady, BASF Bioresearch Corporation, 100 Research Drive, Worcester, MA 01605-4314. Tel.: 508-849-2621; Fax: 508-754-7784.

Abbreviations used: $[Ca^{2+}]_i$, cytosolic free calcium concentration; CICR, calcium-induced calcium release; $Ins(1,4,5)P_3$, inositol 1,4,5-trisphosphate; nrfu, normalized relative fluorescence units; TRH, thyrotropin-releasing hormone.

0006-3495/94/05/1697/09 $2.00

Probes) for 45 min at ambient temperature. Cells were then rinsed with HBSS and maintained in HBSS until use.

Measurement of $[Ca^{2+}]_i$ was performed using an ACAS 570 interactive laser cytometer (Meridian Instruments, Okemos, MI) in the line-scan mode as described previously (Wagner et al., 1993). Briefly, the 488-nm emission of an argon laser was used to excite the calcium-sensitive dye Fluo-3. Fluorescence emission was passed through a 515-nm long-pass filter and monitored using a photomultiplier tube. The computer-controlled microscope stage was moved linearly in 0.6-μm steps so that the laser traced a line across the cell. At each step, 8 fluorescence values were averaged and recorded. The cell average relative fluorescence value at each time point was calculated as the integral of the average of all fluorescence measurements recorded across the cell divided by the length of the scan. A single scan across a cell required approximately 17 ms, and 0.2 s was required to reset the microscope stage. Fluorescence scans were therefore repeated at 0.3-s intervals.

Population selection

Fluorescence records from 540 individual cells were examined using the program CaScan (Brady et al., manuscript in preparation). Cells demonstrating at least 10 spikes in the absence of any drug treatment were included in the study (353 cells). The mean signal/noise ratio of cell records in this subpopulation was 8.7. Unless otherwise stated, all data and statistics represent properties of cell calcium profiles in the absence of drug treatment.

Normalization procedure and relationship of normalized fluorescence to $[Ca^{2+}]_i$

Background fluorescence was recorded from the coverslip area adjacent to each cell and subtracted from each point in the cell's fluorescence record. All fluorescence records were normalized such that the mean fluorescence value before any drug treatment was set equal to 1.0 normalized relative fluorescence unit (nrfu). Since no cellular autofluorescence was observed in the Fluo-3 emission wavelength region, and since factors causing calcium-independent variation in fluorescence magnitude (e.g., amount of Fluo-3 loaded and cell morphology) affected mean fluorescence proportionately, normalization should, on average, remove contributions of such factors to the fluorescence records. Because the baseline $[Ca^{2+}]_i$ varies from cell to cell, it was not possible to evaluate absolute $[Ca^{2+}]_i$ in the individual cells. It was possible, however, to correlate the mean fluorescence observed in a large population of cells with the mean $[Ca^{2+}]_i$ measured by an alternative technique. Mean baseline $[Ca^{2+}]_i$ was measured in populations of GH_4C_1 cells loaded with the dye Fura-2 as described previously (Tornquist and Tashjian, 1989). Eleven independent measurements yielded a basal $[Ca^{2+}]_i$ of 180 ± 100 nM (mean ± SD).

Defining F_{max} as the maximal fluorescence signal observable if $[Ca^{2+}]_i$ for the population is much greater than K_d of the dye, then

$$F_{max} = \frac{F_{mean}(K_d + [Ca]_{i,mean})}{[Ca]_{i,mean}} \quad (1)$$

where $[Ca]_{i,mean}$ is the mean cytosolic free calcium concentration in a population of cells, K_d is the dissociation constant of Fluo-3 (450 nM; Tsien, 1989), and F_{mean} is the mean fluorescence value in a population of cells. *Note:* Eq. 1 is a rearranged version of the binding hyperbola

$$F_{mean} = F_{max}\frac{[Ca]_{i,mean}}{K_d + [Ca]_{i,mean}}$$

Spike baseline can then be expressed in terms of $[Ca^{2+}]_i$:

$$[Ca]_{base} = \frac{F_{base} \cdot K_d}{F_{max} - F_{base}} \quad (2)$$

where F_{base} is the population mean spike baseline fluorescence. Spike amplitude, which is defined as the magnitude of change in fluorescence above the spike baseline ($F_{peak} - F_{base}$, or ΔF), can be expressed as a change in $[Ca^{2+}]_i$:

$$\Delta[Ca] = \frac{(\Delta F + F_{base})K_d}{F_{max} - (\Delta F + F_{base})} - [Ca]_{base} \quad (3)$$

Composite spike profiles and calculation of average spike profiles

Spikes were identified using the program CaScan, and spike-recognition criteria were developed as described (Brady et al., manuscript in preparation). Composite spike plots were prepared by subtracting the spike baseline from the fluorescence values of all data points in the spike (thereby moving all spikes to a common baseline of 0) and plotting the spikes on a common time axis such that all spike maxima occurred at $t = 0$. Average spike profiles were calculated from the arithmetic mean fluorescence values of all spikes at each time point; after termination of the record of each spike, the final observed fluorescence value for that spike was used for calculation of subsequent average fluorescence for the population of spikes. The time derivative of an average spike profile was calculated as:

$$\left(\frac{\Delta F}{\Delta t}\right)_t = \frac{F_{t_+} - F_t}{t_+ - t}$$

where F_t is the fluorescence value at time t, and t_+ is the next sample time (i.e., $t_+ = t + 0.3$ s).

Statistical methods

Non-linear regression analyses were performed using the curve-fitting functions of Sigmaplot (Jandel Scientific, Corte Madera, CA), which are based on the Levenberg-Marquardt algorithm. Linear regressions were performed by standard methods. To estimate the significance of correlations, the t statistic was calculated from the correlation coefficient (R^2) and the number of data points (n):

$$t = \sqrt{\frac{R^2(n-2)}{1-R^2}}$$

p values corresponding to t and n were then obtained from a two-tailed t-distribution table (Croxton, 1953).

RESULTS AND DISCUSSION

Spike decay is approximated by a biphasic exponential decay model

Fig. 1 (*top, inset*) shows a portion of a cell fluorescence record containing numerous spikes. Although the decay of many of these spikes was interrupted by the onset of another spike, spikes which were not interrupted could be used to examine the nature of the decay process. The spike marked by an asterisk was replotted on an expanded time scale (Fig. 1, *top*). Relative fluorescence was measured every 0.3 s, and each point on the expanded plot corresponds to one measurement. The measurements were fitted to a biphasic exponential decay model:

$$F(t) = F_0 + F_1 \exp^{-t/\tau} + F_2 \exp^{-t/\tau_{slow}} \quad (4)$$

where F_0 represents the baseline fluorescence, F_1 represents the magnitude of a rapidly decaying (time constant τ) fluorescence component, and F_2 is the magnitude of a slowly

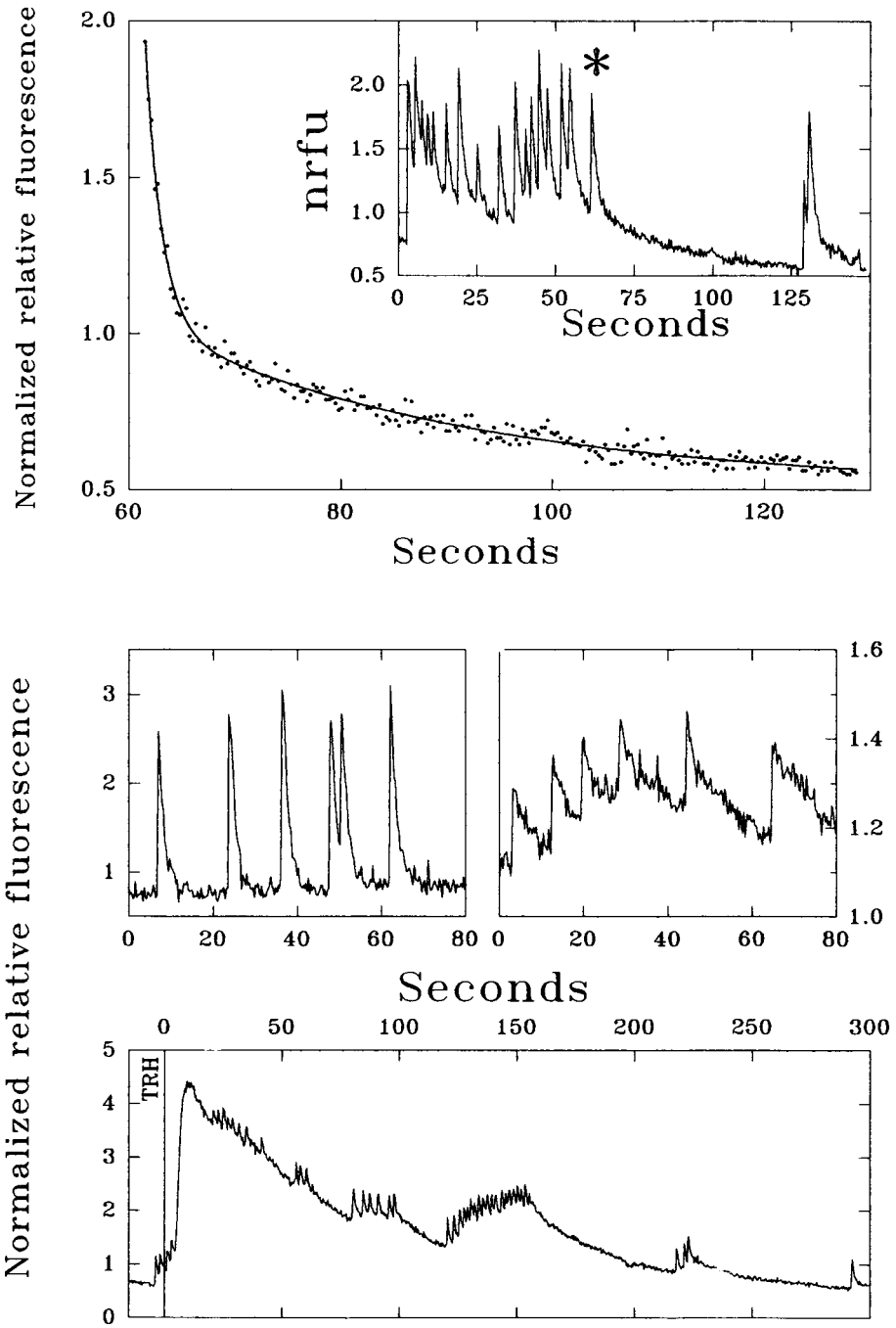

FIGURE 1 Spike decay is described by a biphasic exponential. (*Top, inset*) Portion of a cell fluorescence record showing numerous calcium spikes. The falling phase of the spike marked by * was replotted on a magnified time scale (*top*). The solid curve represents the best fit by non-linear regression to Eq. 4, using parameters $F_0 = 0.50$ nrfu, $F_1 = 0.91$ nrfu, $\tau = 0.64$ s, $F_2 = 0.52$ nrfu, and $\tau_{slow} = 0.033$ s. (*Middle, left*) Portion of a cell fluorescence record showing spikes that lack the slow phase of decay. (*Middle, right*) Portion of a cell fluorescence record showing spikes that lack the fast phase of decay. (*Bottom*) Cell fluorescence record showing spikes superimposed on the slow decay of a large calcium transient generated by treatment with 100 nM TRH at $t = 0$ (vertical line marked TRH).

decaying (time constant τ_{slow}) fluorescence component. The function accurately models the decay of this particular spike, identifying distinct rapid and slow processes with time constants of 0.64 s^{-1} ($t_{1/2} = 1.1$ s) and 0.033 s^{-1} ($t_{1/2} = 21$ s), respectively. The magnitude of the rapid phase was nearly twice as large as that of the slow phase.

We frequently found that the slow phase of decay was less apparent than that shown in Fig. 1 (*top*), i.e., that spikes returned quickly to baseline. One such example is shown in Fig. 1 (*middle, left*). Rarely, the fast phase of decay was absent or diminutive, as shown in Fig. 1 (*middle, right*). As demonstrated below, the goodness of fit to an exponential

model shown in Fig. 1 (*top*) was not universally observed; a simple exponential decay model often approximated but did not exactly describe the fast phase of decay.

The kinetics of spike decay suggest the existence of at least two calcium removal processes which have time constants that can differ by as much as 20-fold. Further insight into these processes was gained by examining spikes superimposed on the slow calcium removal induced after treatment of cells with thyrotropin-releasing hormone (TRH). Fig. 1 (*bottom*) shows a fluorescence record from a cell treated at $t = 0$ with TRH, which caused release of calcium from inositol-1,4,5-trisphosphate ($Ins(1,4,5)P_3$)-sensitive intracellular stores into the cytosol (Albert and Tashjian, 1984; Lucas et al., 1985). $[Ca^{2+}]_i$ was maximal within 10 s of TRH addition and then slowly returned to the initial baseline level. Spikes superimposed on this slow decay of $[Ca^{2+}]_i$ were of similar appearance and kinetics to spikes occurring after $[Ca^{2+}]_i$ returned to the initial baseline level. In addition, numerous spikes occurring within a short time period (e.g., between $t = 120$ and 160 s) caused the slowly decaying fluorescence to become elevated. Both fast and slow processes were therefore observed to occur simultaneously and independently.

Observation of rapid spikes superimposed on top of a slowly decaying signal stimulated, for example, by treatment with TRH, may indicate the presence of two compartments of calcium which are in communication. The slower time constant of the target "pool" for TRH suggests that this pool is of relatively high capacity (i.e., physically larger and/or more strongly buffered). In contrast, the lower-capacity pool is susceptible to rapid transients, the decay of which may lead to a small increase in the fluorescence of the larger pool. In Fig. 1 (*bottom*), this small increase (between $t = 120$ and 160 s) was cumulative when numerous rapid spikes occurred in succession. Thus, in this cell, the smaller pool apparently adjoined and emptied into the larger pool; in other cells, the relative pool capacities and the state of the barrier separating the pools may have differed, leading to the variable patterns shown in Fig. 1 (*middle*). Since the rapid calcium transients have been correlated with the occurrence of calcium action potentials (Schlegel et al., 1987), the smaller "pool" is likely to be located near to the plasma membrane. The larger pool may be located more interior to the cell, where it would remain accessible to a rapidly diffusing messenger such as $Ins(1,4,5)P_3$ (Allbritton et al., 1992).

Calcium removal mechanisms that could account for the decay of fast calcium spikes include calcium diffusion and rapid sequestration by cytosolic calcium buffers (Allbritton et al., 1992), uptake or efflux by calcium pumps (Petersen et al., 1993), and extrusion by sodium/calcium exchangers. The fast phase of spike decay was not slowed when sodium was replaced by choline in the extracellular buffer (K. Wagner, unpublished observations), indicating that sodium/calcium exchange was not a major factor in the rapid decay process. The fast decay phase was not affected by thapsigargin, an inhibitor of intracellular Ca^{2+}-ATPases that are responsible for refilling $Ins(1,4,5)P_3$-sensitive calcium stores in GH_4C_1 cells (Law et al., 1990; Tanaka and Tashjian, 1993). A thapsigargin-insensitive calcium pool is proposed to be an important regulator of $[Ca^{2+}]_i$ in these cells, and thapsigargin-insensitive plasma membrane calcium ATPases could rapidly pump calcium into the extracellular buffer. The action of calcium pumps is unlikely to account entirely for the fast decay of spikes, however, since the independence of the fast and slow processes (Fig. 1, *bottom*) suggests that they act on functionally distinct calcium pools and that some fraction of the rapidly removed calcium is convertible to the slowly removed form.

A rapid decay process involving diffusion of calcium, proposed to account for the time course of calcium spikes in pancreatic β-cells (Sherman et al., 1990; Rorsman et al., 1992), could also account for our findings. Calcium entering the cell via opening of calcium channels during an action potential could cause a transient localized increase in $[Ca^{2+}]_i$, saturating all available Fluo-3 within a discrete subplasmalemmal domain. Calcium would then diffuse (Allbritton et al., 1992) into the general cytosol, becoming diluted as the domain expanded, but also encountering more Fluo-3 with which it could combine to generate a fluorescence signal. There would thus occur a lag between the initial influx event and the occurrence of a maximal fluorescence signal, the duration of which would depend on the diffusion properties of the cytosol. Calcium would continue to diffuse until it was homogeneously distributed throughout the cytosol, from which it would be removed by slower pump or exchange mechanisms. Thus, both the rise and decay phases of calcium spikes could be affected by the calcium diffusion characteristics of any given cell. It was important, therefore, to examine closely factors affecting the kinetics of the rising and rapid falling phases of calcium spikes.

τ increases directly with spike amplitude

In Fig. 2 (*top*), 102 spikes recorded from a single cell were replotted such that spike maxima were aligned at $t = 0$. The group of spikes with normalized amplitudes <1.2 nrfu occurred spontaneously, while the spikes of amplitude >1.2 nrfu occurred after treatment of the cell with Bay K 8644, a voltage-gated calcium channel agonist (Schramm et al., 1983). The thick line represents the mean profile obtained by averaging the fluorescence values of *all* spikes at each time point. Strikingly, the profiles of the falling phases of the spikes were parallel, i.e., they did not converge with time. τ for each peak was estimated by linearizing the falling phase of each spike and performing linear regression analysis:

$$\mathrm{Ln}(F) = \mathrm{Ln}(F_{peak}) - \frac{t}{\tau} \quad (5)$$

τ was found to increase with spike amplitude over a wide amplitude range (Fig. 2, *bottom*). Notably, τ was not constant (i.e., spikes of greater magnitude decayed more slowly than spikes of lesser magnitude) for spikes occurring either before or after Bay K treatment. Further, whereas spikes simulated using a simple exponential decay model and a constant τ of

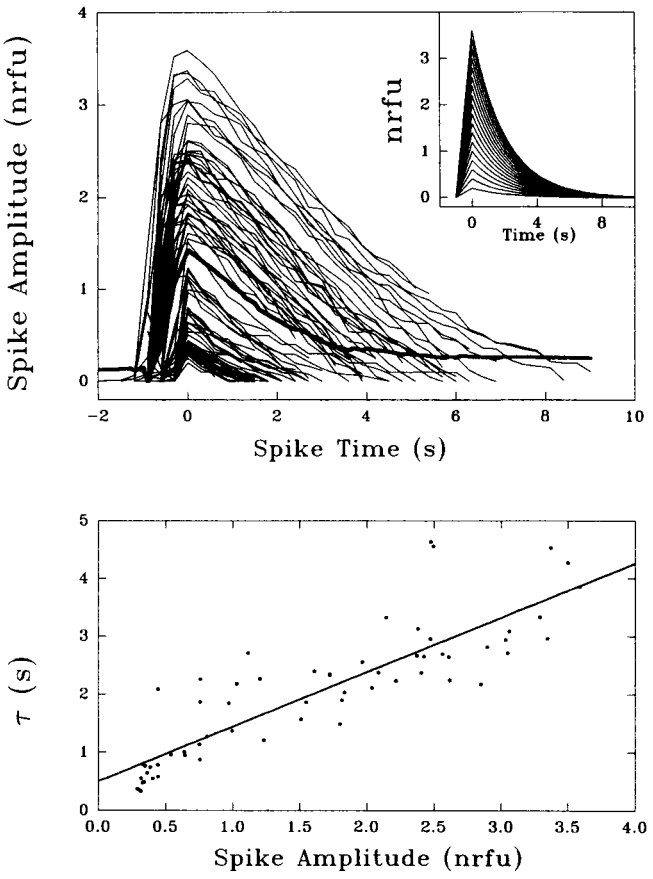

FIGURE 2 The rapid spike decay time constant, τ, increases with spike amplitude. (*Top*) Composite plot of all spikes in a record from an individual cell before and after treatment with Bay K 8644. Spikes of amplitude <1.2 nrfu occurred before Bay K treatment, while spikes of amplitude >1.2 nrfu were stimulated by the calcium channel agonist. The thick line represents the average spike profile, which was obtained by averaging the fluorescence of all spikes at each time point. (*Inset*) Simulated profiles of spikes using a single exponential decay model and constant $\tau = 2.0$ s (see text). (*Bottom*) Eq. 5 was used to linearize the falling phase of the spikes in the major upper panel, and linear regression analysis was used to estimate τ for each spike. The straight line, representing the least squares best fit, has a slope of 0.78 s/nrfu and a correlation coefficient R^2 of 0.95.

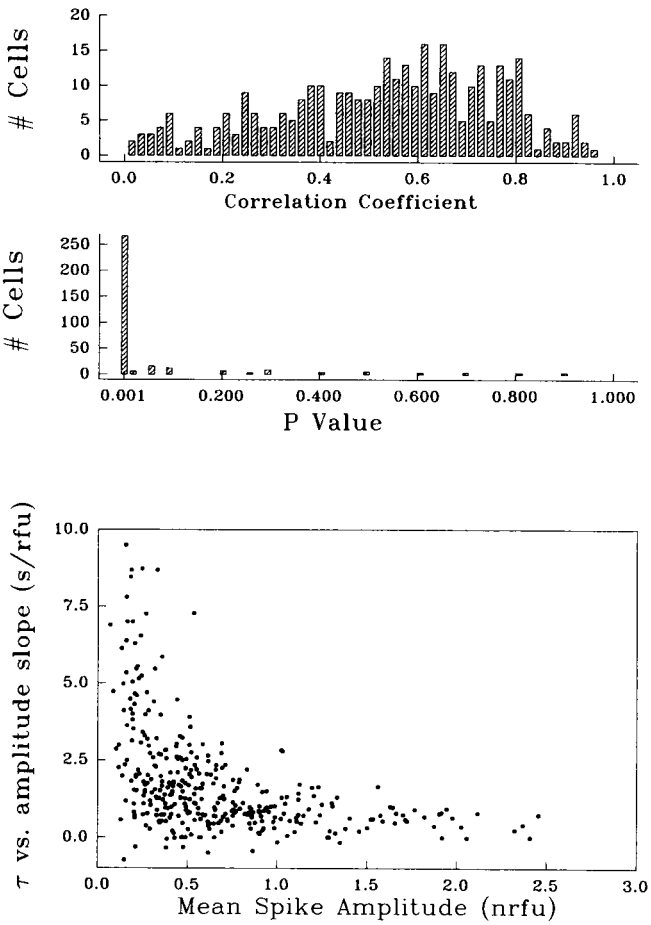

FIGURE 3 Dependence of τ on spike amplitude is inversely related to mean spike amplitude. For each of 353 untreated cells, τ versus spike amplitude plots were generated (see Fig. 2, *bottom*), and linear regression analysis was used to evaluate the slope, correlation coefficient, and p value for the relationship. (*Top*) Correlation coefficients ranged from 0 to 0.96; the mean was 0.60. (*Middle*) p values indicated a high probability of significance ($p < 0.05$) for 80% of the regressions. (*Bottom*) The slope of the τ versus amplitude plots varied inversely with the mean spike amplitude.

2.0 s converged at longer times (Fig. 2, *top, inset*), the experimental spikes did not converge, due to the positive correlation of τ with spike amplitude. Therefore, higher amplitude spikes had relatively prolonged decay phases. While use of Bay K-treated cells demonstrated that this phenomenon occurred over a wide range of spike amplitudes, the positive correlation between τ and spike amplitude was observed in >80% of the untreated cells in this study (see Figs. 3 and 5). It has been proposed that calcium-induced calcium release (CICR) accounts for some fraction of the total calcium comprising these calcium spikes (Wagner et al., 1993). The involvement of CICR is consistent with a positive correlation between τ and spike amplitude; greater peak $[Ca^{2+}]_i$ should induce further calcium release and thereby sustain the spike decay phase. For each cell the slope of the τ versus spike amplitude plot (Fig. 2, *bottom*) would then be a measure of the degree of involvement of CICR in the calcium spikes of that cell.

Alternatively, a positive correlation between τ and spike amplitude could occur if a calcium uptake or efflux mechanism (e.g., a calcium ATPase) became saturated at high $[Ca^{2+}]_i$. Spikes of higher amplitude would be broadened by an increasing inability of the cell to remove calcium rapidly. The validity of this hypothesis was evaluated by examining the relationships among τ, spike amplitude, and mean spike amplitude in a large number of individual cells.

The τ versus spike amplitude slope varies inversely with mean spike amplitude

We used Eq. 5 and linear regression analysis to examine the correlation between τ and spike amplitude in 353 untreated cells (Fig. 3). The quality of the regression analyses is indicated in the top and middle panels. The correlation coefficient of the regression line varied from 0 to 0.96, with a mean value of 0.60. The t-test indicated that the correlations were, in general, highly significant with $p < 0.01$ for 80% of

the cells. In Fig. 3 (*bottom*) the *slope* of each cell's τ versus amplitude plot (as defined in Fig. 2, *bottom*) was plotted as a function of the cell's mean spike amplitude, and a striking inverse relationship was found. This relationship was not strict, however. Among cells of low mean spike amplitude, the dependence of τ on spike amplitude was found to vary over a wide range, from weak to strong; among cells with large mean spike amplitude, this dependence was always relatively weak.

The results shown in Fig. 3 are not consistent with the hypothesis that the positive correlation between τ and spike amplitude (Fig. 2, *bottom*) occurred due to saturation of a calcium removal mechanism, because that hypothesis predicts that the strength of the correlation should *increase* at high mean spike amplitudes. In contrast, Fig. 3 (*bottom*) clearly demonstrates a decrease at high mean spike amplitudes. We therefore propose that the reciprocal relationship between the τ versus amplitude slope and the mean spike amplitude may be related to the involvement of CICR, as follows. It has been proposed (Wagner et al., 1993) that CICR requires *both* calcium influx through L-type calcium channels *and* a responsive CICR-related calcium store. Cells that have active CICR and small or modest spike amplitudes are therefore likely to exhibit a strong dependence of τ on spike amplitude. At higher $[Ca^{2+}]_i$, however, the contribution of CICR is expected to diminish, due either to emptying of the CICR store during a high-amplitude event, or to saturation of calcium binding sites involved in triggering the CICR response. Cells with depleted or inactive CICR stores should show a weak dependence of τ on spike amplitude irrespective of the mean amplitude.

Mean spike rise and fall times correlate strongly with τ and weakly with mean spike amplitude

If calcium diffusion has a significant role in determining the kinetics of the calcium spikes, then the diffusion properties of cytosolic calcium would be expected to affect the durations of both the rising and falling phases of spikes. We therefore examined in a population of 353 individual cells the correlations of the mean spike rise-time and fall-time with each other, with mean τ, and with mean spike amplitude. Correlation coefficients and estimated significance levels are reported in Table 1. Both mean rise time and mean fall time correlated better with τ than with mean spike amplitude. Furthermore, mean rise time correlated better with mean fall time than with mean spike amplitude. These results suggest that there was some factor(s) that influenced the kinetic properties of spikes (i.e., rise time, fall time, and τ) independently of the spike amplitude. CICR could contribute significantly to the kinetics of both rising and falling phases of the spikes, but it should then contribute significantly to the amplitude. Alternatively, if diffusion were responsible for the lag between transient calcium influx and generation of a maximal fluorescence signal, then both phases of a spike should be affected independently of amplitude. Thus, the durations of both the rising and falling phases of spikes in a given cell are likely to be influenced by the cell's cytosolic calcium diffusion properties. Thus, the mean value of τ for any particular cell could be influenced by at least two factors: cytosolic calcium diffusion and the degree of involvement of CICR in calcium spikes.

TABLE 1 Correlation coefficients relating mean spike rise time, fall time, τ, and amplitude in a population of 353 individual GH_4C_1 cells*

Measurement	Correlation coefficient with τ	Amplitude	Fall time
Rise time	0.48‡	0.10	0.40‡
Fall time	0.84‡	0.48‡	

* Mean values of spike rise time, fall time, τ, and amplitude in individual cells were plotted pairwise and analyzed by linear regression analysis. The table reports correlation coefficients and estimated statistical significance of the correlation for each pair of spike parameters.
‡ $p < 0.001$.

Spike amplitudes and τ are log-normally distributed

Fig. 4 (*top*) shows the distribution of spike amplitudes among a population of 353 untreated cells. The distribution was log-normal, with a mean amplitude of 0.45 nrfu (i.e., 0.45 times the mean cell fluorescence), and a 2.15-fold standard deviation. By equating the mean fluorescence of this population of single cells with the mean basal $[Ca^{2+}]_i$ of large populations of GH_4C_1 cells (see Materials and Methods), the mean spike amplitude was estimated (Eq. 3) to be 141 nM. The mean spike maximum (net $[Ca^{2+}]_i$ at the top of spikes) was estimated to be 306 nM, which is significantly less than the 606 nM previously reported (Schlegel et al., 1987). We attribute this difference to our inclusion of weakly spiking cells, which were likely excluded from studies based on many fewer cells (Schlegel et al., 1987). The distribution of τ (Fig. 4, *bottom*) was also log-normal, with a mean of 0.78 s and a 1.73-fold standard deviation. Since log-normal distributions arise when deviations from the mean accumulate multiplicatively (c.f. normal distributions arise when deviations accumulate *additively*) we postulate that the spikes may arise from a process involving positive feedback, such that an initial event may be amplified. The fold-amplification may then vary with the event size and other complex variables determining the responsiveness of a given cell. Concurrently or alternatively, a calcium sensor involved in spike generation might respond not to $[Ca^{2+}]_i$ directly, but to the logarithm of $[Ca^{2+}]_i$. An example of such a sensor is the $Ins(1,4,5)P_3$ receptor, of which the channel-opening probability has the form of a smooth bell-shaped curve when plotted as a function of Log([Ca]) (Bezprozvanny et al., 1991).

Fig. 4 (*middle*) shows the distributions of spike amplitudes in four individual GH_4C_1 cells. The amplitude range of spikes in any single cell was only a fraction of the entire range observed in the population. Similarly, spike fall times in

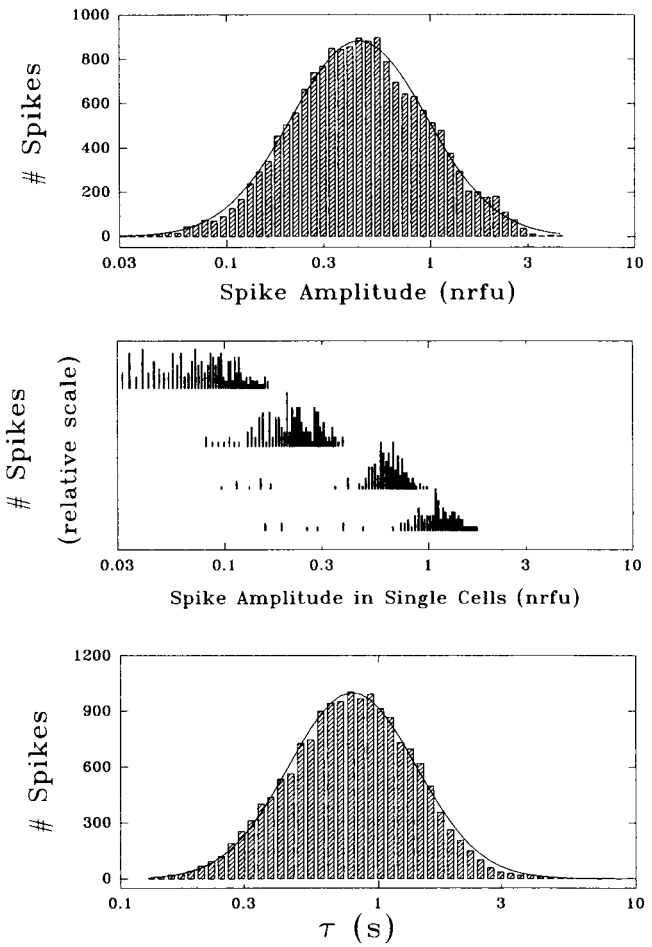

FIGURE 4 Distribution of spike amplitudes and τ in the population and in selected single cells. (*Top*) Spike amplitude histogram of 16,431 spikes in 353 cells. The smooth curve represents the nonlinear least squares best fit to a log-normal model with a mean of 0.45 nrfu and a 2.15-fold standard deviation. (*Middle*) Distributions of spike amplitudes in four selected single cells plotted on the same abscissa as the population histogram, showing the relative span of amplitudes in individual cells. (*Bottom*) Equation [2] was applied to estimate τ for 15,854 spikes in 353 cells, and the results were plotted as a histogram. The smooth curve represents the nonlinear least squares best fit to a log-normal model with a mean of 0.78 s and a 1.73-fold standard deviation.

single cells occurred over only a portion of the entire range observed in the population (data not shown). Both spike amplitude and spike kinetics remained stable for the duration (150–700 s) of these observations.

Spike shape is a unique property of each cell

In the spike profiles shown in Fig. 2 (*top*) it can be observed that many spikes were slightly "flattened" at their peaks, i.e., that early in the falling phase the rate of decrease was less than would be predicted by a simple exponential decay model. Spike flattening could arise from several sources. First, saturation of Fluo-3 by high $[Ca^{2+}]_i$ could result in large changes in $[Ca^{2+}]_i$ at spike maxima with little or no fluorescence change. Second, flattening could represent an experimental artifact introduced by the 0.3 s sampling rate, if the time of the true spike maximum occurred within a window of ± 0.3 s around the apparent spike maximum. Third, flattening could result from CICR, as discussed above, or from delayed onset of an elimination mechanism that contributes to the decay phase of spikes.

Several lines of evidence suggest that spike flattening was due neither to dye saturation nor to experimental artifact. First, the distribution of spike amplitudes in the population of single cells (Fig. 4, *top*) indicated that the mean spike maximum represented a $[Ca^{2+}]_i$ of 306 nM, which is insufficient to saturate Fluo-3 (K_d = 450 nM). Second, if dye saturation were the primary cause of spike flattening in any given cell, then the degree of flattening should increase with spike amplitude. Fig. 5 shows composite spike profiles from a cell with little spike "flattening" (*top*) and a cell with substantial spike "flattening" (*middle*). A quantitative parameter

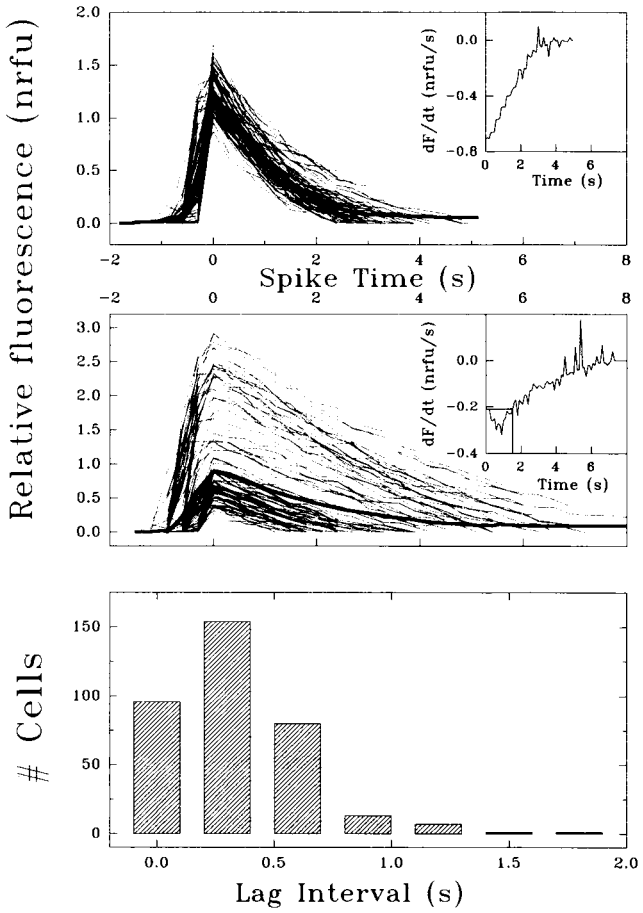

FIGURE 5 Composite spike plots illustrating spike "flattening" and histogram of mean lag interval in a population of single cells. (*Top*) Composite spike plot from a single cell with little "flattening." The thick line represents the composite average spike profile. (*Inset*) The composite average spike profile was numerically differentiated with respect to time, and *dF/dt* was plotted as a function of time. (*Middle*) Composite spike plot from a single cell with significant "flattening." The thick line represents the composite average spike profile. (*Inset*) The composite average spike profile was numerically differentiated with respect to time, and *dF/dt* was plotted as a function of time. Lag interval was defined as the time required to recover to the value of *dF/dt* at $t = 0$. (*Bottom*) Distribution of lag intervals in a population of 353 untreated single cells.

that describes the degree of spike "flattening" may be obtained by numerically differentiating the falling phase of an average spike profile and plotting the first derivative (dF/dt) as a function of time (Fig. 5, *insets*). The average profile of the first cell behaved like a simple exponential decay, in that the first derivative increased smoothly from a negative value toward 0. In contrast, the cell with "flattened" spikes showed a lag of 1.5 s during which the first derivative decreased (see boxed area, Fig. 5, *middle inset*) before increasing toward 0.

Using this method, lag intervals were evaluated for the 353 cells in our study. Fig. 5 (*bottom*) shows the distribution of lag times among these cells. Significant correlation was observed between lag interval and mean fall time ($R^2 = 0.41$) or mean τ ($R^2 = 0.40$, data not shown), whereas lag time was poorly correlated with mean spike amplitude ($R^2 = 0.17$, data not shown). Further evidence for the lack of correlation between spike flattening and spike amplitude was obtained from detailed study of composite spike profiles such as those shown in Fig. 5 (*middle*). For each cell, individual calcium spikes of all amplitudes shared a similar profile, and flattening was therefore a cellular characteristic which affected both low- and high-amplitude spikes. Finally, if spike flattening were an experimental artifact introduced by discrete sampling, then flattening (and "sharpening") should affect spikes randomly, and should neither affect the average profile obtained from many individual spikes nor produce lag times in excess of 0.3 s. We conclude that the profiles of both low- and high-amplitude spikes were a unique characteristic of each individual cell, and were likely related to the activity levels of CICR and/or calcium pumping mechanisms in each cell. A unique cellular spike-decay profile or "calcium signature" has been described in several cell types, including hepatocytes (Prentki et al., 1988) and insulinoma cells (Rooney et al., 1989). It should be noted, however, that the latter observations pertain to the relatively slow decay of agonist-stimulated calcium spikes, as opposed to the rapid, spontaneous spikes described in the present study.

Effects of buffering by Fluo-3

Calcium indicator dyes are strong calcium buffers that could alter the nature of intracellular calcium events. We used several approaches to examine the degree to which cellular Fluo-3 content might have contributed to our observations. First, we examined calcium spikes in cells loaded using either 3 μM Fluo-3 (14 cells, 1218 spikes) or 18 μM Fluo-3 (10 cells, 694 spikes) (c.f., the majority of cells in our study were loaded using 9 μM Fluo-3). No significant differences in mean spike amplitude, kinetics, or frequency were observed between these test populations (data not shown). Second, since the mean basal fluorescence value used to normalize each fluorescence record should account for factor(s) related to dye content, variation in spike parameters with the normalization factor should indicate the degree of artifact introduced by the Fluo-3 itself. We observed a weak but significant *negative* correlation between the normalization factor and mean spike amplitude ($R^2 = 0.18$; data not shown). Although the calcium dye Fura-2 has been shown to accelerate the rate of calcium diffusion through *Xenopus* oocyte cytoplasm (Allbritton et al., 1992), we observed no significant correlation between the normalization factor and any kinetic parameter, including spike rise time, fall time, and τ (data not shown). High dye concentrations may therefore have caused minor suppression of calcium spike amplitude, probably through the buffering action of Fluo-3, but were unlikely to have introduced artifacts into experimental measurements of spike rise time, fall time, and τ.

CONCLUSIONS

Although spontaneous rapid calcium fluctuations in GH_4C_1 cells may be initiated by action potentials (Schlegel et al., 1987), the fluctuations evolve and decay with a time course much slower than that of action potentials. We have used statistical techniques to examine the relationships between amplitudes and the kinetic properties of spontaneous spikes in individual cells. Spike decay was best modeled as a biphasic exponential, suggesting that at least two kinetically distinct processes exist by which calcium is removed from the cytoplasm. Furthermore, these processes were observed to occur independently and simultaneously. The fast decay time constant, τ, increased with the spike amplitude, indicating that some process, possibly CICR, prolonged spikes in a calcium-dependent fashion. In a population of 353 cells, the mean spike rise time and mean spike fall time were correlated independently of spike amplitude. These observations are consistent with a model in which an influx of calcium accumulates transiently in small sub-plasmalemmal domains, spreads through the cytosol by diffusion, and then triggers CICR to an extent that varies substantially from cell to cell.

We thank Patrick W. Yacono for assistance in data collection and analysis, Yuji Tanaka for discussions of calcium spike mechanisms, and Jean Foley for assistance in the preparation of this manuscript.

This work was supported in part by research grants from the National Institutes of Health (DK-11011 to A.H.T. and HL-32854 to D.E.G.) and by a Postdoctoral Fellowship (Award PF-3356) from the American Cancer Society to K.D.B.

REFERENCES

Albert, P. R., and A. H. Tashjian Jr. 1984. Thyrotropin-releasing hormone-induced spike and plateau in cytosolic free Ca^{2+} concentrations in pituitary cells. Relation to prolactin release. *J. Biol. Chem.* 259:5827–5832.

Allbritton, N. L., T. Meyer, and L. Stryer. 1992. Range of messenger action of calcium ion and inositol 1:4,5-trisphosphate. *Science.* 258:1812–1815.

Berridge, M. J. 1993. Inositol trisphosphate and calcium signalling. *Nature.* 361:315–325.

Bezprozvanny, I., J. Watras, and B. E. Ehrlich. 1991. Bell-shaped calcium-response curves of $Ins(1,4,5)P_3$- and calcium-gated channels from endoplasmic reticulum of cerebellum. *Nature.* 351:751–754.

Chiavaroli, C., D. M. F. Cooper, C. L. Boyajian, R. Murray-Whelan, N. Demaurex, A. M. Spiegel, and W. Schlegel. 1992. Spontaneous intracellular calcium oscillations and $G_s\alpha$ subunit expression are inversely correlated with secretory granule content in pituitary cells. *J. Neuroendocrinol.* 4:473–481.

Croxton, F. E. 1953. Elementary Statistics. Dover Publications, Inc., New York.

Law, G. J., J. A. Pachter, O. Thastrup, M. R. Hanley, and P. S. Dannies. 1990. Thapsigargin, but not caffeine, blocks the ability of thyrotropin-releasing hormone to release Ca^{2+} from an intracellular store in GH_4C_1 pituitary cells. *Biochem. J.* 267:359–364.

Lucas, D. O., S. M. Bajjalieh, J. A. Kowalchyk, and T. F. J. Martin. 1985. Direct stimulation by thyrotropin-releasing hormone (TRH) of polyphosphoinositide hydrolysis in GH_3 cell membranes by a guanine nucleotide-modulated mechanism. *Biochem. Biophys. Res. Commun.* 132:721–728.

Ostlund, R. E., Jr., J. T. Leung, S. V. Hajek, T. Winokur, and M. Melman. 1978. Acute stimulated hormone release from cultured GH_3 pituitary cells. *Endocrinology.* 103:1245–1252.

Ozawa, S., and N. Kimura. 1979. Membrane potential changes caused by thyrotropin-releasing hormone in the clonal GH_3 cell and their relationship to secretion of pituitary hormone. *Proc. Natl. Acad. Sci. USA.* 76: 6017–6020.

Pachter, J. A., G. J. Law, and P. S. Dannies. 1988. TRH and Bay K 8644 synergistically stimulate prolactin release but not $^{45}Ca^{2+}$ uptake. *Am. J. Physiol.* 255:C633-C640.

Petersen, C. C. H., O. H. Petersen, and M. J. Berridge. 1993. The role of endoplasmic reticulum calcium pumps during cytosolic calcium spiking in pancreatic acinar cells. *J. Biol. Chem.* 268:22262–22264.

Prentki, M., M. C. Glennon, A. P. Thomas, R. L. Morris, F. M. Matschinsky, and B. E. Corkey. 1988. Cell-specific patterns of oscillating free Ca^{2+} in carbamylcholine-stimulated insulinoma cells. *J. Biol. Chem.* 263:11044–11047.

Rooney, T. A., E. J. Sass, and A. P. Thomas. 1989. Characterization of cytosolic calcium oscillations induced by phenylephrine and vasopressin in single Fura-2-loaded hepatocytes. *J. Biol. Chem.* 264:17131–17141.

Rorsman, P., C. Ämmälä, Per-O. Berggren, K. Bokvist, and O. Larsson. 1992. Cytoplasmic calcium transients due to single action potentials and voltage-clamp depolarization in mouse pancreatic B-cells. *EMBO J.* 11: 2877–2884.

Schlegel, W., B. P. Winiger, P. Mollard, P. Vacher, F. Wuarin, G. R. Zahnd, C. B. Wollheim, and B. Dufy. 1987. Oscillations of cytosolic Ca^{2+} in pituitary cells due to action potentials. *Nature.* 329:719–721.

Schramm, M., G. Thomas, R. Towart, and G. Franckowiak. 1983. Novel dihydropyridines with positive inotropic action through activation of Ca^{2+} channels. *Nature.* 303:535–537.

Sherman, A., J. Keizer, and J. Rinzel. 1990. Domain model for Ca^{2+}-inactivation of Ca^{2+} channels at low channel density. *Biophys. J.* 58: 985–995.

Simasko, S. M. 1991. Reevaluation of the electrophysiological actions of thyrotropin-releasing hormone in a rat pituitary cell line (GH_3). *Endocrinology.* 128:2015–2026.

Stojilkovic, S. S., and K. J. Catt. 1992. Calcium oscillations in anterior pituitary cells. *Endocr. Rev.* 13:256–280.

Tanaka, Y., and A. H. Tashjian Jr. 1993. Functional identification and quantitation of three intracellular calcium pools in GH_4C_1 cells: evidence that the caffeine-responsive pool is coupled to a thapsigargin-resistant ATP-dependent process. *Biochemistry.* 32:12062–12073.

Taraskevich, P. S., and W. W. Douglas. 1980. Electrical behaviour in a line of anterior pituitary cells (GH cells) and the influence of the hypothalamic peptide, thyrotrophin releasing factor. *Neuroscience.* 5:421–431.

Tashjian, A. H., Jr. 1979. Clonal strains of hormone-producing pituitary cells. *Methods Enzymol.* 58:527–535.

Tashjian, A. H., Jr., Y. Yasumura, L. Levine, G. H. Sato, and M. L. Parker. 1968. Establishment of clonal strains of rat pituitary tumor cells that secrete growth hormone. *Endocrinology.* 82:342–352.

Tornquist, K., and A. H. Tashjian, Jr. 1989. Dual actions of 1:25-dihydroxycholecalciferol on intracellular Ca^{2+} in GH_4C_1 cells: evidence for effects on voltage-operated Ca^{2+} channels and Na^+/Ca^{2+} exchange. *Endocrinology.* 124:2765–2776.

Tsien, R. Y. 1989. Fluorescent probes of cell signaling. *Annu. Rev. Neurosci.* 12:227–253.

Wagner, K. A., P. W. Yacono, D. E. Golan, and A. H. Tashjian, Jr. 1993. Mechanism of spontaneous intracellular calcium fluctuations in single GH_4C_1 rat pituitary cells. *Biochem. J.* 292:175–182.

White, B. A., L. R. Bauerle, and F. C. Bancroft. 1981. Calcium specifically stimulates prolactin synthesis and messenger RNA sequences in GH_3 cells. *J. Biol. Chem.* 256:5942–5945.